Instantons in lepton pair production

Brandenburg, A.; Ringwald, A.; Utermann, A.

published in
Nuclear Physics B
2006

DOI (link to publisher)
10.1016/j.nuclphysb.2006.07.020

document version
Publisher's PDF, also known as Version of record

Available online at www.sciencedirect.com
ScienceDirect
ELSEVIER
Nuclear Physics B 754 (2006) 107–126
NUCLEAR PHYSICS B

Instantons in lepton pair production

Arnd Brandenburg [a,1], Andreas Ringwald [a], Andre Utermann [b,*]

[a] *Deutsches Elektronen-Synchrotron DESY, Hamburg, Germany*
[b] *Department of Physics and Astronomy, Vrije Universiteit Amsterdam, The Netherlands*

Received 31 May 2006; received in revised form 3 July 2006; accepted 12 July 2006

Available online 7 August 2006

Abstract

We consider QCD instanton-induced contributions to lepton pair production in hadron–hadron collisions. We relate these contributions to those known from deep inelastic scattering and demonstrate that they can be calculated reliably for sufficiently large momentum transfer. We observe that the instanton contribution to the angular distribution of the lepton pairs at finite momentum transfer strongly violates the Lam–Tung relation—a relation between coefficient functions of the angular distribution which is valid within the framework of ordinary perturbation theory. The drastic violation of this relation, as seen in experimental data, might be related to such instanton-induced effects.

1. Introduction

The Standard Model of electroweak (quantum flavor dynamics (QFD)) and strong (QCD) interactions is extraordinarily successful. This success is largely based on the possibility to apply ordinary perturbation theory to the calculation of hard, short-distance dominated scattering processes, since the relevant gauge couplings are small. Certain processes, however, cannot be described by ordinary perturbation theory, no matter how small the gauge coupling is. These processes are associated with axial anomalies [1] and manifest themselves as anomalous violation of baryon plus lepton number $(B + L)$ in QFD and chirality (Q_5) in QCD [2]. They are induced by topological fluctuations of the non-Abelian gauge fields, notably by instantons [3].

* Corresponding author.
E-mail address: utermann@few.vu.nl (A. Utermann).
[1] Present address: Genedata AG, Maulbeerstraße 46, CH-4016 Basel, Switzerland.

0550-3213/$ – see front matter
doi:10.1016/j.nuclphysb.2006.07.020

A number of nonperturbative issues in the Standard Model can be understood in terms of such topological fluctuations and the associated anomalous processes. On the one hand, QCD instantons seem to play an important role in various long-distance aspects of QCD, such as providing a possible solution to the axial $U(1)$ problem [2] or being at work in chiral symmetry breaking [4]. In QFD, on the other hand, analogous topological fluctuations of the gauge fields and the associated $B + L$ violating processes are very important at high temperatures [5] and have therefore a crucial impact on the evolution of the baryon and lepton asymmetries of the universe [6].

Are manifestations of such topological fluctuations also directly observable in high-energy scattering processes? This question has been seriously considered in the late 1980s, originally in the context of QFD [7]. But, despite considerable theoretical [8] and phenomenological [9] efforts, the actual size of the cross-sections in the relevant, tens of TeV energy regime was never established (for recent attempts, see Ref. [10]). Meanwhile, the focus switched to quite analogous QCD instanton-induced hard scattering processes in deep inelastic scattering [11], which are calculable from first principles within instanton-perturbation theory [12], yield sizeable rates for observable final state signatures in the fiducial regime of the latter [13,14], and are actively searched for at HERA [15]. Moreover, it has been argued that larger-size QCD instantons, beyond the semiclassical, instanton-perturbative regime, may well be responsible for the bulk of inelastic hadronic processes and build up soft diffractive scattering [16]. It was emphasized for the first time in Ref. [17] that single photon or single W production at large transverse momentum offers a possibility to study QCD instanton-induced effects from first principles at the LHC. Unlike the processes considered in the present paper, the dominant subprocess for this dedicated instanton search at high energies at the LHC [17,18] is induced by gluon fusion, e.g., $gg \to V + X$, $V = \gamma^* \to \ell^+\ell^-$. Moreover, the kinematical region is remarkable different from our region of interest, i.e., the available transverse momenta and virtualities are significantly larger than those we concentrate on throughout this paper.

In this paper, we consider QCD instanton-induced contributions to lepton pair production in hadron–hadron collisions[2] (cf. Fig. 1). We relate these contributions to the ones previously calculated for deep inelastic scattering [12], thereby demonstrating that the former—like the latter—can be calculated from first principles. In particular, as already emphasized in Ref. [17], the typical inverse hard transverse momentum scale $q_\perp^{-1}$ in lepton pair production provides a dynamical infrared cutoff for the instanton size parameter ρ, thereby allowing for a controlled semiclassical approximation, which rests on the smallness of the QCD coupling at the effective momentum scale $1/\langle\rho\rangle$: $\alpha_s(1/\langle\rho\rangle) \ll 1$. Hence, in addition to deep inelastic scattering, lepton

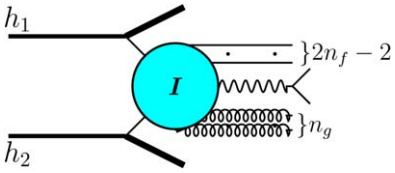

Fig. 1. QCD instanton-induced contribution to lepton pair production in hadron–hadron collisions, $h_1 + h_2 \to (n_f - 1)[\bar{q}_R + q_R] + \ell^+ + \ell^- + n_g g + X$, corresponding to n_f light flavours.

[2] This is often called the Drell–Yan process [19]. Instanton contributions to this process have been first discussed in Ref. [20] at a qualitative level.

pair production at large transverse momentum may be viewed as a distinguished process for studying manifestations of QCD instantons.

We put special emphasis on the angular distribution of the lepton pairs at finite momentum transfer. We observe that the instanton contribution strongly violates the Lam–Tung relation [21] between coefficient functions of the angular distribution, which has been verified within the framework of ordinary perturbation theory—the QCD improved parton model—up to $\mathcal{O}(\alpha_s^2)$ [22,23] and even holds for the inclusion of parton transverse momentum and soft gluon effects [24,25]. Indeed, it has been argued that the drastic violation of this relation, as seen in experimental data [26–28], might be due to a nontrivial structure of the QCD vacuum [22], and in particular could be related to instanton-induced effects [29].

The outline of this paper is as follows: in Section 2 we introduce the instanton-induced contribution to lepton pair production. Afterwards we review the known results in the related process in DIS in an instanton background. The crucial part of this section is the continuation of these results to hadron collisions which leads us to the photon production tensor on partonic level. In Section 3 we will use these results to calculate the angular distribution of the produced leptons on the partonic (Section 3.1) and the hadronic (Section 3.2) level. In Section 3.3 we give an outlook on the inclusion of multi gluon processes which lead to an enhancement of the instanton contributions. We present our conclusions in Section 4.

2. From deep inelastic scattering to lepton pair production

We start with the derivation of the instanton-induced contribution to lepton pair production on the parton level. We will concentrate on the case with quarks in the initial state. These contributions dominate over the ones involving initial state gluons, at least for scattering processes where valence-like quarks and antiquarks contribute, e.g., in $p\bar{p}$ or $\pi^{\pm}N$ collisions. This is certainly different at very high energies where very small parton momentum fractions x dominate. Since the lower bound on x is set by M^2/S, where M^2 is the invariant mass squared of the lepton pair and S is the hadron–hadron center of mass energy squared, the contributing values of x considered in our study are not so small for our chosen values of M^2 and S, see Section 3.2. For the main case of phenomenological interest, i.e., $n_f = 3$ light flavours ($m_q \langle\rho\rangle \ll 1$, for $q = u, d, s$), instanton-induced quark–antiquark annihilation involves in the final state at least two quarks and two antiquarks of different flavour, such that the chirality is violated by $2n_f = 6$ [2], plus an arbitrary number of gluons (g), e.g., (cf. Fig. 2)

$$\begin{aligned} u_L + \bar{u}_L &\to \gamma^* + \bar{d}_R + d_R + \bar{s}_R + s_R + n_g g \\ &\hookrightarrow \ell^+ + \ell^-. \end{aligned} \tag{1}$$

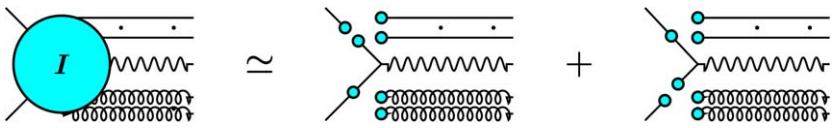

Fig. 2. Instanton-induced process for $n_f = 3$, $u_L + \bar{u}_L \to \gamma^* + \bar{d}_R + d_R + \bar{s}_R + s_R + n_g g$, in leading semiclassical approximation. The amplitude involves the products of the appropriate classical fields (lines ending at blobs: fermionic zero modes (straight) and instanton gauge fields (curly)) as well as the nonzero mode quark propagator in the instanton background (quark line with central blob).

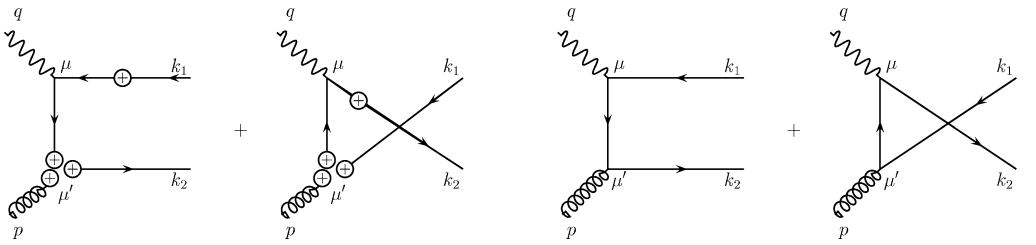

Fig. 3. Instanton-induced process for $n_f = n_g = 1$, $\gamma^*(q) + g(p) \to \bar{q}_R(k_1) + q_R(k_2)$, in leading semiclassical approximation (left) and the analogous process, $\gamma^*(q) + g(p) \to \bar{q}_R(k_1) + q_L(k_2)$, from ordinary perturbation theory (right). Both figures from Ref. [12].

The amplitudes for the related processes in deep inelastic scattering,

$$\gamma^* + g \to \bar{u}_R + u_R + \bar{d}_R + d_R + \bar{s}_R + s_R + (n_g - 1)g, \tag{2}$$

have been derived, in leading-order semiclassical approximation, in Ref. [12]. For clarity and simplicity, let us concentrate here on the explicit result for the simplest appropriate[3] case $n_f = n_g = 1$ (cf. Fig. 3 (left)),

$$\begin{aligned}
&\mathcal{T}^a_{\mu\mu'}\big(\gamma^*(q) + g(p) \to \bar{q}_R(k_1) + q_R(k_2)\big) \\
&\quad = -\mathrm{i}e_q\lambda^a \frac{\sqrt{2}}{8}\pi^3 d\left(\frac{2\pi}{\alpha_s(\mu_r)}\right)^{13/2} \exp\left[-\frac{2\pi}{\alpha_s(\mu_r)}\right] 2^b \Gamma\left(\frac{b+1}{2}\right)\Gamma\left(\frac{b+3}{2}\right) \\
&\qquad \times \chi_R^\dagger(k_2)\big[(\sigma_{\mu'}\bar{p} - p\bar{\sigma}_{\mu'})v(q,k_1;\mu_r)\bar{\sigma}_\mu - \sigma_\mu \bar{v}(q,k_2;\mu_r)(\sigma_{\mu'}\bar{p} - p\bar{\sigma}_{\mu'})\big]\chi_L(k_1),
\end{aligned} \tag{3}$$

with the four-vector v_λ,

$$v_\lambda(q,k;\mu_r) \equiv \frac{1}{\mu_r}\left\{\left[\frac{(q-k)_\lambda}{-(q-k)^2} + \frac{k_\lambda}{2q\cdot k}\right]\left(\frac{\mu_r^2}{-(q-k)^2}\right)^{\frac{b+1}{2}} - \frac{k_\lambda}{2q\cdot k}\left(\frac{\mu_r^2}{-q^2}\right)^{\frac{b+1}{2}}\right\}, \tag{4}$$

and confront it with its chirality conserving counterpart from ordinary perturbation theory (cf. Fig. 3 (right)),

$$\begin{aligned}
&\mathcal{T}^a_{\mu\mu'}\big(\gamma^*(q) + g(p) \to \bar{q}_R(k_1) + q_L(k_2)\big) \\
&\quad = e_q g_s \frac{\lambda^a}{2}\chi_L^\dagger(k_2)\left[\bar{\sigma}_{\mu'}\frac{(q-k_1)}{(q-k_1)^2}\bar{\sigma}_\mu - \bar{\sigma}_\mu\frac{(q-k_2)}{(q-k_2)^2}\bar{\sigma}_{\mu'}\right]\chi_L(k_1).
\end{aligned} \tag{5}$$

Here, e_q is the quark charge in units of the electric charge e, g_s is the strong coupling, λ^a, $a = 1,\ldots,8$, are the Gell-Mann $SU(3)$ generators, and μ and μ' are the four-vector indices of the photon and gluon, respectively (cf. Fig. 3). The two-component Weyl-spinors $\chi_{L,R}$ in Eqs. (3) and (5) satisfy the Weyl-equations, $\bar{k}\chi_L(k) = 0$, $k\chi_R(k) = 0$, and the relations $\chi_L(k)\chi_L^\dagger(k) = k$, $\chi_R(k)\chi_R^\dagger(k) = \bar{k}$. We used the abbreviations, $k \equiv k_\mu\sigma^\mu$, $\bar{k} \equiv k_\mu\bar{\sigma}^\mu$, for any four-vector k_μ, with the familiar σ-matrices, $\sigma_\mu = (1,\vec{\sigma})$ and $\bar{\sigma}_\mu = (1,-\vec{\sigma})$, with $\vec{\sigma}$ being the Pauli matrices.

[3] Note that the even simpler case $n_g = 0$ is not relevant for us, since the corresponding process in lepton pair production would contribute only at vanishingly small transverse momentum where, anyhow, instanton perturbation theory is not applicable (see below).

The other parameters in Eq. (3) arose from (the integration over) the instanton size distribution [2,30], whose two-loop renormalization group improved form [31],

$$D(\rho,\mu_r)=\frac{d}{\rho^5}\left(\frac{2\pi}{\alpha_s(\mu_r)}\right)^6\exp\left[-\frac{2\pi}{\alpha_s(\mu_r)}\right](\rho\mu_r)^{\beta_0+\frac{\alpha_s(\mu_r)}{4\pi}(\beta_1-12\beta_0)}, \tag{6}$$

has been exploited, where μ_r is the renormalization scale and

$$\alpha_s(\mu_r)\equiv\frac{g_s^2(\mu_r)}{4\pi}=\frac{4\pi}{\beta_0\ln\left(\frac{\mu_r^2}{\Lambda^2}\right)}\left[1-\frac{\beta_1}{\beta_0^2}\frac{\ln\left(\ln\left(\frac{\mu_r^2}{\Lambda^2}\right)\right)}{\ln\left(\frac{\mu_r^2}{\Lambda^2}\right)}\right] \tag{7}$$

is the strong fine structure constant at two-loop, with

$$\beta_0=11-\frac{2}{3}n_f,\qquad \beta_1=102-\frac{38}{3}n_f \tag{8}$$

being the familiar perturbative coefficients of the QCD beta-function. The constant d is given by

$$d=\frac{C_1}{2}\mathrm{e}^{-3C_2+n_fC_3}, \tag{9}$$

with $C_1=0.466$, $C_2=1.51$, and $C_3=0.292$, in the $\overline{\mathrm{MS}}$-scheme [32–34]. The variable b in Eq. (3) is a shorthand for the effective power of $\rho\mu_r$ in the instanton size distribution (6),

$$b\equiv\beta_0+\frac{\alpha_s(\mu_r)}{4\pi}(\beta_1-12\beta_0). \tag{10}$$

It is important to note that the perturbative expression (6) for the size distribution is valid for small $\rho\Lambda\ll 1$ where Λ is the fundamental scale in QCD. Indeed, a comparison with lattice data from quenched ($n_f=0$) QCD [35] yields $\rho\Lambda\lesssim 0.4$ for the fiducial region of instanton perturbation theory [36]. This can be translated into a fiducial kinematical region for instanton perturbation theory in deep inelastic scattering. On account of the fact that the main contribution to the integration over the instanton size comes from [12]

$$\langle\rho\rangle\simeq\frac{b+3/2}{\sqrt{-q^2}},\ \frac{b+3/2}{\sqrt{-(q-k_1)^2}},\ \frac{b+3/2}{\sqrt{-(q-k_2)^2}}, \tag{11}$$

corresponding to different terms in Eqs. (3) and (4), one has to require that all virtualities, $\sqrt{-q^2}$, $\sqrt{-(q-k_1)^2}$, and $\sqrt{-(q-k_2)^2}$, exceed $\mathcal{Q}_{\min}\approx(4-6)$ GeV, in order to stay in the realm of instanton perturbation theory.

It is now straightforward to obtain the corresponding amplitudes relevant for lepton pair production via quark–antiquark annihilation, namely the one for the chirality violating instanton-induced process $q_L(k_1)+\bar{q}_L(k_2)\to\gamma^*(q)+g(p)$ (cf. Fig. 4) and the one for the analogous ordinary perturbative process $q_L(k_1)+\bar{q}_R(k_2)\to\gamma^*(q)+g(p)$. In fact, these processes are basically T-conjugates of the deep inelastic processes from Eqs. (3) and (5), and the respective

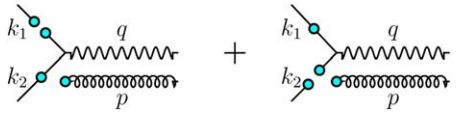

Fig. 4. Instanton-induced process for $n_f=n_g=1$, $q_L(k_1)+\bar{q}_L(k_2)\to\gamma^*(q)+g(p)$, in leading semiclassical approximation.

modulus-squared amplitudes are therefore identical, up to reflections of three-momenta. Some care has of course to be taken with respect to the photon virtuality: whereas in deep inelastic scattering it is space-like, $Q^2 \equiv -q^2 > 0$, in lepton pair production it is time-like, $M^2 \equiv q^2 > 0$. We will comment on this later.

We have calculated the contribution of our simple processes to the partonic tensor[4] for inclusive quark–antiquark annihilation into a virtual photon,

$$w_{\mu\nu}(k_1, k_2; q) = \sum_{n=0}^{\infty} w_{\mu\nu}^{(n)}(k_1, k_2; q), \tag{12}$$

$$w_{\mu\nu}^{(n)}(k_1, k_2; q) = \frac{1}{4\pi} \int \mathrm{dPS}^{(n)}\, \mathcal{T}_\mu(k_1, k_2; q, p_1, \ldots, p_n) \mathcal{T}_\nu^*(k_1, k_2; q, p_1, \ldots, p_n), \tag{13}$$

$$\int \mathrm{dPS}^{(n)} = \prod_{j=1}^{n} \int \frac{\mathrm{d}^4 p_j}{(2\pi)^3} \delta^{(+)}\big(p_j^2\big) (2\pi)^4 \delta^{(4)}(k_1 + k_2 - q - p_1 - \cdots - p_n). \tag{14}$$

Following Ref. [21], this tensor can be decomposed as

$$w_{\mu\nu} = -\tilde{g}_{\mu\nu} w_1 + \tilde{K}'_\mu \tilde{K}'_\nu w_2 - \frac{\tilde{K}'_\mu \tilde{k}'_\nu + \tilde{K}'_\nu \tilde{k}'_\mu}{2} w_3 + \tilde{k}'_\mu \tilde{k}'_\nu w_4, \tag{15}$$

with $K' = k_1 + k_2$, $k' = k_1 - k_2$, $\tilde{g}_{\mu\nu} = g_{\mu\nu} - q_\mu q_\nu / q^2$, $\tilde{K}'_\mu = \tilde{g}_{\mu\nu} K'^\nu / \sqrt{s}$, and $\tilde{k}'_\mu = \tilde{g}_{\mu\nu} k'^\nu / \sqrt{s}$, where $s = (k_1 + k_2)^2$. In turn, the different w_i can be obtained,

$$w_i = p^i_{\mu\nu} w^{\mu\nu}, \quad i = 1, 2, 3, 4, \tag{16}$$

from the partonic tensor with the help of the following projectors,

$$p^0_{\mu\nu} = -g_{\mu\nu}, \tag{17}$$

$$p^1_{\mu\nu} = \frac{4}{stu} \varepsilon_{\mu\rho\sigma\tau} k_1^\rho k_2^\sigma q^\tau \varepsilon_{\nu\rho'\sigma'\tau'} k_1^{\rho'} k_2^{\sigma'} q^{\tau'}, \tag{18}$$

$$p^2_{\mu\nu} = \frac{-q^2 s}{tu} \big[\tilde{k}'^2 \big(p^0_{\mu\nu} - 2p^1_{\mu\nu}\big) + \tilde{k}'_\mu \tilde{k}'_\nu\big], \tag{19}$$

$$p^3_{\mu\nu} = \frac{-2q^2 s}{tu} \left[(\tilde{k}' \cdot \tilde{K}') \big(p^0_{\mu\nu} - 2p^1_{\mu\nu}\big) + \frac{\tilde{k}'_\mu \tilde{K}'_\nu + \tilde{K}'_\mu \tilde{k}'_\nu}{2}\right], \tag{20}$$

$$p^4_{\mu\nu} = \frac{-q^2 s}{tu} \big[\tilde{K}'^2 \big(p^0_{\mu\nu} - 2p^1_{\mu\nu}\big) + \tilde{K}'_\mu \tilde{K}'_\nu\big], \tag{21}$$

where $t = (q - k_1)^2$ and $u = (q - k_2)^2$. We are especially interested in the contribution $w^{(1)}_{\mu\nu}$ to $w_{\mu\nu}$ (12),

$$w'_{\mu\nu} = \overline{\sum}_{\text{spins,colours}} \mathcal{T}_\mu(k_1, k_2; q, p) \mathcal{T}_\nu^*(k_1, k_2; q, p), \qquad w'_i = p^i_{\mu\nu} w'^{\mu\nu}, \tag{22}$$

$$\begin{aligned} w_i^{(1)} &= \frac{1}{4\pi} \int \frac{\mathrm{d}^4 p}{(2\pi)^3} \delta^{(+)}\big(p^2\big) (2\pi)^4 \delta^{(4)}(k_1 + k_2 - q - p) w'_i \\ &= \frac{1}{2} \delta^{(+)}\big((k_1 + k_2 - q)^2\big) w'_i. \end{aligned} \tag{23}$$

[4] Averaging over colour and spin of the initial state is implicitly understood in Eq. (12); the index n is to label besides the final state partons also their spin and colour degrees of freedom.

Along these lines, we find that the simple instanton-induced process $q_L + \bar{q}_L \to \gamma^* + g$ contributes as follows to the functions w_i',

$$
\begin{aligned}
-g^{\mu\nu} w_{\mu\nu}^{(\mathrm{I})\prime} &= \xi^{(\mathrm{I})} \biggl\{ \left(\frac{M^2}{-t}\right)^{b+1} + \left(\frac{M^2}{-u}\right)^{b+1} + \frac{2tu}{(t-M^2)(u-M^2)} \\
&\quad \times \biggl[\left(\frac{M^2}{-t}\right)^{\frac{b+1}{2}} \left(\frac{M^2}{-u}\right)^{\frac{b+1}{2}} + 1 \\
&\quad - \operatorname{Re}(-1)^{\frac{b+1}{2}} \left(\left(\frac{M^2}{-t}\right)^{\frac{b+1}{2}} + \left(\frac{M^2}{-u}\right)^{\frac{b+1}{2}} \right) \biggr] \biggr\}, \qquad (24)
\end{aligned}
$$

$$
w_1^{(\mathrm{I})\prime} = \frac{\xi^{(\mathrm{I})}}{2} \left\{ \left(\frac{M^2}{-t}\right)^{\frac{b+1}{2}} + \left(\frac{M^2}{-u}\right)^{\frac{b+1}{2}} \right\}^2, \qquad (25)
$$

$$
\begin{aligned}
w_2^{(\mathrm{I})\prime} &= \frac{\xi^{(\mathrm{I})}}{2} \biggl\{ -\frac{sM^2}{(t-M^2)^2} \left(\frac{M^2}{-t}\right)^{b+1} - \frac{sM^2}{(u-M^2)^2} \left(\frac{M^2}{-u}\right)^{b+1} + \frac{tu(t-u)^2}{(t-M^2)^2(u-M^2)^2} \\
&\quad - \frac{sM^2(4M^2 s + t^2 + u^2)}{tu(t-M^2)(u-M^2)} \left(\frac{M^2}{-t}\right)^{\frac{b+1}{2}} \left(\frac{M^2}{-u}\right)^{\frac{b+1}{2}} + \frac{(t-u)\operatorname{Re}(-1)^{\frac{b+1}{2}}}{(t-M^2)^2(u-M^2)^2} \\
&\quad \times \biggl[\bigl(t-M^2\bigr)\bigl(2M^4 - M^2 t - tu - 3M^2 u + u^2\bigr) \left(\frac{M^2}{-u}\right)^{\frac{b+1}{2}} \\
&\quad - \bigl(u-M^2\bigr)\bigl(2M^4 - M^2 u - tu - 3M^2 t + t^2\bigr) \left(\frac{M^2}{-t}\right)^{\frac{b+1}{2}} \biggr] \biggr\}, \qquad (26)
\end{aligned}
$$

$$
\begin{aligned}
w_3^{(\mathrm{I})\prime} &= \xi^{(\mathrm{I})} \biggl\{ \frac{sM^2}{(t-M^2)^2} \left(\frac{M^2}{-t}\right)^{b+1} - \frac{sM^2}{(u-M^2)^2} \left(\frac{M^2}{-u}\right)^{b+1} - \frac{(s+M^2)(t-u)tu}{(t-M^2)^2(u-M^2)^2} \\
&\quad + \frac{sM^2(s+M^2)(t-u)}{(t-M^2)(u-M^2)tu} \left(\frac{M^2}{-t}\right)^{\frac{b+1}{2}} \left(\frac{M^2}{-u}\right)^{\frac{b+1}{2}} - \frac{\operatorname{Re}(-1)^{\frac{b+1}{2}}}{(t-M^2)^2(u-M^2)^2} \\
&\quad \times \biggl[\bigl(t-M^2\bigr)\bigl(2M^6 - 2M^4 t - 4M^4 u + M^2 t^2 + 3M^2 u^2 + t^2 u - u^3\bigr) \left(\frac{M^2}{-u}\right)^{\frac{b+1}{2}} \\
&\quad - \bigl(u-M^2\bigr)\bigl(2M^6 - 2M^4 u - 4M^4 t + M^2 u^2 \\
&\quad + 3M^2 t^2 + tu^2 - t^3\bigr) \left(\frac{M^2}{-t}\right)^{\frac{b+1}{2}} \biggr] \biggr\}, \qquad (27)
\end{aligned}
$$

$$
\begin{aligned}
w_4^{(\mathrm{I})\prime} &= \frac{\xi^{(\mathrm{I})}}{2} \biggl\{ -\frac{sM^2}{(t-M^2)^2} \left(\frac{M^2}{-t}\right)^{b+1} - \frac{sM^2}{(u-M^2)^2} \left(\frac{M^2}{-u}\right)^{b+1} + \frac{tu(s+M^2)^2}{(t-M^2)^2(u-M^2)^2} \\
&\quad - \frac{sM^2(t^2+u^2)}{tu(t-M^2)(u-M^2)} \left(\frac{M^2}{-t}\right)^{\frac{b+1}{2}} \left(\frac{M^2}{-u}\right)^{\frac{b+1}{2}} + \frac{(s+M^2)\operatorname{Re}(-1)^{\frac{b+1}{2}}}{(t-M^2)^2(u-M^2)^2} \\
&\quad \times \biggl[\bigl(t-M^2\bigr)\bigl(-M^2 u + M^2 t + tu + u^2\bigr) \left(\frac{M^2}{-u}\right)^{\frac{b+1}{2}} \\
&\quad + \bigl(u-M^2\bigr)\bigl(-M^2 t + M^2 u + tu + t^2\bigr) \left(\frac{M^2}{-t}\right)^{\frac{b+1}{2}} \biggr] \biggr\}, \qquad (28)
\end{aligned}
$$

where

$$\xi^{(\mathrm{I})} \equiv \pi^2 e_q^2 \mathcal{N}^2 \left(\frac{2\pi}{\alpha_s(\mu_r)}\right)^{13} \exp\left(-\frac{4\pi}{\alpha_s(\mu_r)}\right)\left(\frac{\mu_r^2}{M^2}\right)^b \frac{s}{M^2}, \tag{29}$$

$$\mathcal{N} \equiv \frac{1}{2}\pi^2 d 2^b \Gamma\left(\frac{b+1}{2}\right)\Gamma\left(\frac{b+3}{2}\right). \tag{30}$$

We have obtained these results starting from Eq. (3), contracting it with the gluon polarization vector $\epsilon^{\mu'}(p)$ and taking the modulus squared, exploiting FORM [37] for the spinor traces. The results (24)–(28) for the contribution of our simple instanton-induced process to the partonic tensor for inclusive quark–antiquark annihilation into a time-like photon look quite similar to the contribution of the analogous simple instanton-induced process to the deep inelastic structure tensor of a gluon found in Ref. [12]. A notable difference is the appearance of the factor $\mathrm{Re}(-1)^{(b+1)/2}$, which reduces to unity in the space-like kinematics of deep inelastic scattering and was therefore not visible in the results of Ref. [12]. On the other hand, the full instanton contribution to the deep inelastic structure tensor of a gluon can be obtained from Eqs. (24)–(28) by replacing the combinatorial factor $1/((2\cdot N_c)^2)$ by $1/(2\cdot(N_c^2-1))$ and by substituting $\mathrm{Re}(-1)^{(b+1)/2}$ by 1.

As a check, let us also quote the corresponding perturbative contributions to the inclusive partonic tensor arising from Eq. (5),

$$-g^{\mu\nu} w_{\mu\nu}^{(\mathrm{pt})\prime} = \xi^{(\mathrm{pt})}\left[\frac{u}{t} + \frac{t}{u} + \frac{2M^2 s}{tu}\right], \tag{31}$$

$$w_1^{(\mathrm{pt})\prime} = -\frac{1}{2} g^{\mu\nu} w_{\mu\nu}^{(\mathrm{pt})\prime}, \tag{32}$$

$$w_2^{(\mathrm{pt})\prime} = -\xi^{(\mathrm{pt})} \frac{sM^2}{tu}, \tag{33}$$

$$w_3^{(\mathrm{pt})\prime} = 0, \tag{34}$$

$$w_4^{(\mathrm{pt})\prime} = w_2^{(\mathrm{pt})\prime}, \tag{35}$$

where

$$\xi^{(\mathrm{pt})} \equiv 2\pi e_q^2 \alpha_s. \tag{36}$$

We obtained this well-known result, see, e.g., [42], by exploiting the same FORM routines as the ones for the instanton-induced contribution, except for replacing the input amplitude (3) by the perturbative amplitude (5).

3. The angular distribution of the lepton pairs

In this section, we will concentrate on the angular distribution of lepton pairs in instanton-induced processes—mainly concentrating on the simple one from the previous section—and compare it to the one predicted from ordinary perturbation theory.

In general, the angular distribution of the charged lepton ℓ^+ in lepton pair production,

$$h_1(K_1) + h_2(K_2) \to \gamma^*(q) + X \hookrightarrow \ell^+(q_+) + \ell^-(q_-) \tag{37}$$

is described by three functions, λ, μ, and ν, which may depend on the kinematic variables of (37),

$$\frac{1}{\sigma}\frac{d\sigma}{d\Omega} = \frac{3}{4\pi}\frac{1}{\lambda+3}\left(1+\lambda\cos^2\theta+\mu\sin 2\theta\cos\phi+\frac{\nu}{2}\sin^2\theta\cos 2\phi\right), \tag{38}$$

θ and ϕ being the polar and azimuthal angles of ℓ^+, respectively [38]. These coefficient functions may be conveniently expressed in terms of hadronic helicity structure functions [39],

$$\lambda = \frac{W_T - W_L}{W_T + W_L}, \tag{39}$$

$$\mu = \frac{W_\Delta}{W_T + W_L}, \tag{40}$$

$$\nu = \frac{2W_{\Delta\Delta}}{W_T + W_L}. \tag{41}$$

Here, we exploit the so-called Collins–Soper frame [38], in which the frame dependent helicity structure functions read, in terms of the hadronic counterparts W_i of the previously introduced invariant functions w_i,

$$W_T = W_1 + \frac{r^2}{2SM^2(1+r^2)}\big[(q\cdot K)^2 W_2 - (q\cdot K)(q\cdot k)W_3 + (q\cdot k)^2 W_4\big], \tag{42}$$

$$W_L = W_1 + \frac{1}{SM^2(1+r^2)}\big[(q\cdot k)^2 W_2 - (q\cdot K)(q\cdot k)W_3 + (q\cdot K)^2 W_4\big], \tag{43}$$

$$W_\Delta = -\frac{r}{SM^2(1+r^2)}\left[-(q\cdot K)(q\cdot k)(W_2+W_4) + \frac{(q\cdot K)^2+(q\cdot k)^2}{2}W_3\right], \tag{44}$$

$$W_{\Delta\Delta} = -\frac{r^2}{2SM^2(1+r^2)}\big[(q\cdot K)^2 W_2 - (q\cdot K)(q\cdot k)W_3 + (q\cdot k)^2 W_4\big], \tag{45}$$

where

$$r^2 \equiv \frac{q_\perp^2}{M^2} = \frac{TU + M^2(M^2 - S - T - U)}{SM^2}, \tag{46}$$

determines the transverse photon momentum $q_\perp$ with respect to the hadronic reaction plane. The kinematic variables $S = (K_1 + K_2)^2$, $T = (q - K_1)^2$ and $U = (q - K_2)^2$ refer to the hadron level (cf. Eq. (37)). Similarly, $K = K_1 + K_2$ and $k = K_1 - K_2$.

3.1. Parton level

The contribution of our simple instanton-induced process as well as the contributions from ordinary perturbation theory to these helicity structure functions are determined by folding their partonic counterparts with the parton density distributions. Before doing that it is instructive to consider first the partonic analogies of the quantities.

Let us start with the contributions arising from ordinary perturbation theory, (cf. Eqs. (31)–(35)),

$$\hat{\lambda}^{(\mathrm{pt})(1)} \equiv \frac{w_T^{(\mathrm{pt})(1)} - w_L^{(\mathrm{pt})(1)}}{w_T^{(\mathrm{pt})(1)} + w_L^{(\mathrm{pt})(1)}} = \frac{2-r^2}{2+3r^2}, \tag{47}$$

$$\hat{\mu}^{(\mathrm{pt})(1)} \equiv \frac{w_\Delta^{(\mathrm{pt})(1)}}{w_T^{(\mathrm{pt})(1)} + w_L^{(\mathrm{pt})(1)}} = \frac{q_\perp}{M}\frac{2s(s+M^2)M^2(t-u)}{(t-M^2)^2+(u-M^2)^2}\frac{1}{2M^2s+3tu}, \tag{48}$$

$$\hat{\nu}^{(\mathrm{pt})(1)} \equiv \frac{2w_{\Delta\Delta}^{(\mathrm{pt})(1)}}{w_T^{(\mathrm{pt})(1)} + w_L^{(\mathrm{pt})(1)}} = \frac{2r^2}{2+3r^2}. \tag{49}$$

In terms of the partonic quantities, the ratio $r^2 = q_\perp^2/M^2$ in Eq. (46) reduces to $tu/(sM^2)$. In particular, we find the Lam–Tung relation [21],

$$1 - \hat{\lambda}^{(\mathrm{pt})(1)} - 2\hat{\nu}^{(\mathrm{pt})(1)} = 0, \tag{50}$$

which, of course, holds also on the hadron level, $1 - \lambda^{(\mathrm{pt})} - 2\nu^{(\mathrm{pt})} = 0$, as long as no intrinsic transverse momentum for the initial state quarks is invoked. It is nearly left intact even if one includes $\mathcal{O}(\alpha_s^2)$ corrections [23].

The contributions arising from our simple instanton-induced process (cf. Eqs. (24)–(28)) are readily calculated along the same lines. They yield quite lengthy expressions, and we do not quote them all analytically, but will illustrate them, instead, graphically. We stress, however, that the Lam–Tung relation is violated by instantons. This is apparent from the following, nonvanishing expression,

$$\begin{aligned} 2\big(w_L^{(\mathrm{I})\prime} - 2w_{\Delta\Delta}^{(\mathrm{I})\prime}\big) = \frac{4\xi^{(\mathrm{I})}tu}{(t-M^2)(u-M^2)} \Bigg\{ 1 - \mathrm{Re}(-1)^{\frac{b+1}{2}} \Bigg[\left(\frac{M^2}{-t}\right)^{\frac{b+1}{2}} + \left(\frac{M^2}{-u}\right)^{\frac{b+1}{2}} \Bigg] \\ - \frac{sM^2}{tu} \left(\frac{M^2}{-t}\right)^{\frac{b+1}{2}} \left(\frac{M^2}{-u}\right)^{\frac{b+1}{2}} \Bigg\}, \end{aligned} \tag{51}$$

for the numerator of the Lam–Tung combination (cf. Eqs. (39)–(41)),

$$1 - \hat{\lambda} - 2\hat{\nu} = \frac{2(w_L - 2w_{\Delta\Delta})}{w_T + w_L}. \tag{52}$$

Note, that the factor $(M^2/\sqrt{tu})^{b+1}$ in the asymmetry (51) arises from a nonplanar diagram. That is in accordance with [29] where the importance of nonplanar interference terms for the violation of the Lam–Tung relation were discussed.

It is useful to view the partonic coefficient functions, for fixed M, as a function of $r = q_\perp/M$ and the partonic Feynman variable

$$x_F \equiv \frac{t-u}{s}. \tag{53}$$

In fact, $\hat{\lambda}$, $\hat{\mu}$, and $\hat{\nu}$ depend, for fixed M, only on r and x_F. Their dependence on these kinematical variables is illustrated in Figs. 5 and 6. We observe the following features:

(i) $\hat{\lambda}$ (top panels) approaches -1 for large r for pure instanton-induced processes (dashed), i.e., these processes tend to be purely longitudinal (cf. Eq. (39)) for large transverse momenta, in contrast to ordinary perturbative processes (dotted and Eq. (47)). The total result for $\hat{\lambda}$ (solid), taking into account both instanton and ordinary processes in the numerator and denominator of the partonic equivalent of Eq. (39), shows little deviation from ordinary perturbation theory. Indeed, there are experimental hints for longitudinally polarized photons in hadron collisions towards larger x_F [28]. Note that, even if the instanton-induced process $q\bar{q} \to \gamma^* g$ is suppressed, for larger x_F, instanton effects might be relevant for this effect since gluon resummation leads to an enhancement in this kinematic region, see Section 3.3.

(ii) The total result (solid) for $\hat{\mu}$ (second panels from top) shows a quite significant deviation from ordinary perturbation theory (dotted) for sizeable x_F and intermediate values of r.

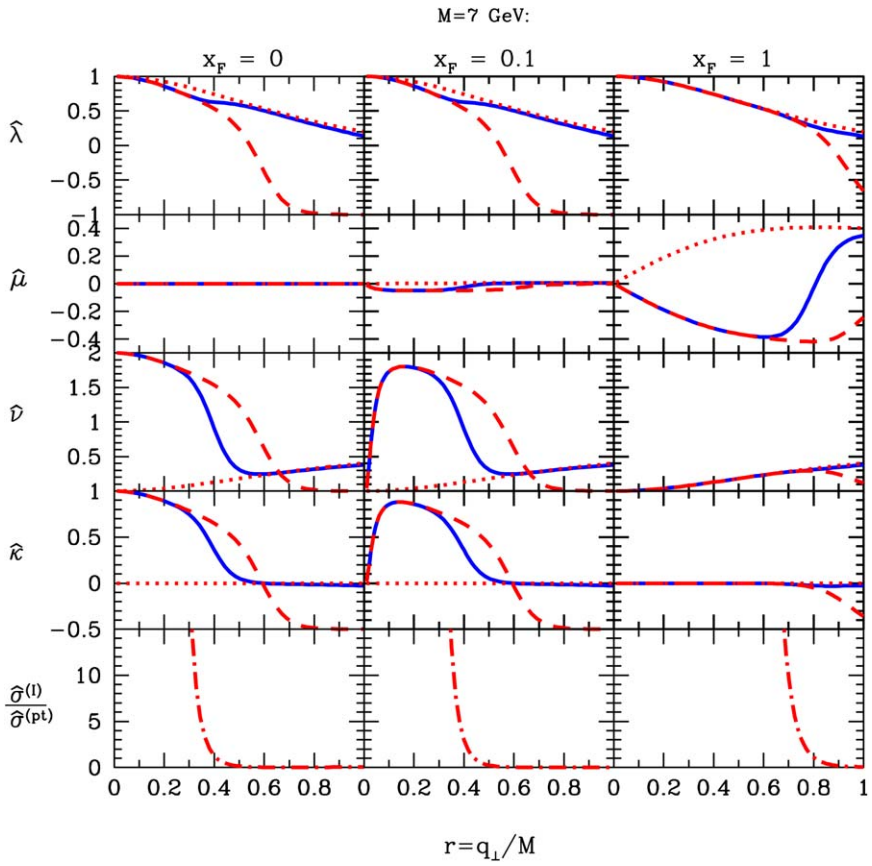

Fig. 5. Coefficient functions of the angular distribution of lepton pairs from quark anti-quark annihilation, as a function of $q_\perp/M$, for various values of x_F, for $M = 7$ GeV. Dotted: result from pure ordinary perturbation theory; dashed: result from pure instanton perturbation theory; solid: total result from ordinary and instanton perturbation theory. Also shown, in the last row, is the ratio of the cross-sections of instanton perturbation theory to ordinary perturbation theory (dashed-dotted). In the numerical results shown we have chosen $\mu_r = M$, $\Lambda = 0.346$ GeV, and $n_f = 3$.

(iii) $\hat{\nu}$ (third panels from top) behaves quite differently in pure instanton-induced processes (dashed) and ordinary perturbative processes (dotted and Eq. (49)). In fact, instanton-induced processes have a value of[5] $\hat{\nu}^{(\mathrm{I})} \approx 2$ at small, but finite r and small x_F, much larger as ordinary perturbative processes ($\hat{\nu}^{(\mathrm{pt})} \ll 1$). Also in the total result for $\hat{\nu}$ (solid) we observe a strong enhancement at small, but finite r and small x_F in comparison to ordinary perturbation theory. Correspondingly, we find a strong violation of the Lam–Tung relation, which we display in the forth panels from top in terms of the parameter

$$\hat{\kappa} \equiv -\frac{1}{4}(1 - \hat{\lambda} - 2\hat{\nu}). \tag{54}$$

[5] In fact, it follows from general arguments [22,29] that as long as instanton processes dominate over ordinary perturbative processes, one expects $\hat{\nu}^{(\mathrm{I})} \approx 2$.

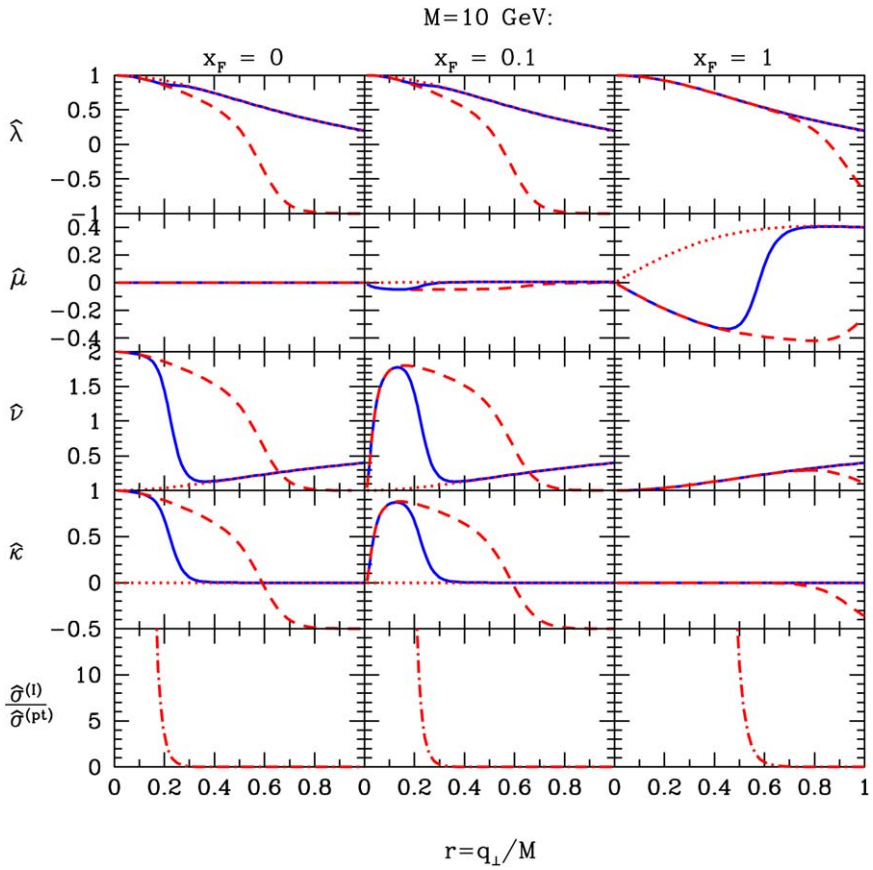

Fig. 6. Same as in Fig. 5, but for $M = 10$ GeV.

Whereas this parameter is identical zero in ordinary perturbative processes (dotted), it is about one, at small r, x_F, for instanton-induced processes, leading to a drastic violation of the Lam–Tung relation in the total result (solid).

(iv) Clearly, instanton effects in the coefficient functions are most visible in kinematical regions where the instanton induced cross-section $\hat{\sigma}^{(\mathrm{I})}$ dominates over the perturbative, $\hat{\sigma}^{(\mathrm{pt})}$, one. The instanton-induced features in Figs. 5 and 6 are indeed located where the ratio (bottom panels; dashed-dotted)

$$\frac{\hat{\sigma}^{(\mathrm{I})}}{\hat{\sigma}^{(\mathrm{pt})}} = \frac{2w_T^{(\mathrm{I})} + w_L^{(\mathrm{I})}}{2w_T^{(\mathrm{pt})} + w_L^{(\mathrm{pt})}} \tag{55}$$

becomes large. Obviously, it gets large towards small momentum transfer. The dominance of instantons is seen to set in like a "brick wall". This sudden onset occurs practically at the boundary of the fiducial kinematical region of instanton perturbation theory, $\sqrt{-t} \approx \mathcal{Q}_{\min}$ or $\sqrt{-u} \approx \mathcal{Q}_{\min}$, for $M > \mathcal{Q}_{\min} \approx (4\text{–}6)$ GeV. Therefore, the instanton features in the coefficient functions at very small momentum transfer, to the left of the sudden onset of instanton dominance in Figs. 5 and 6, lie strictly speaking outside the range of validity of the semiclassical approximation. Fortunately, however, the coefficient functions are *ratios* of helicity structure functions (cf.

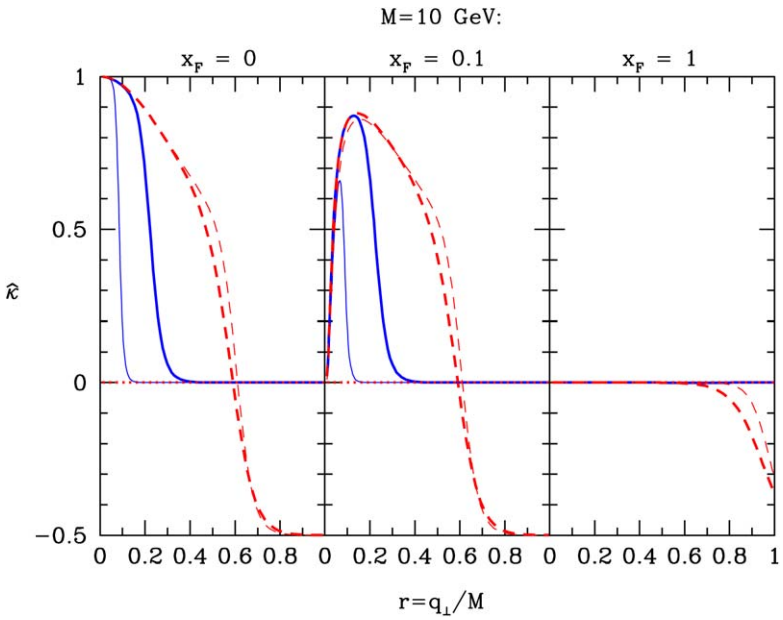

Fig. 7. Illustration of the dependence of our prediction of the Lam–Tung parameter $\hat{\kappa} = \frac{1}{4}(1-\hat{\lambda}-2\hat{\nu})$ on the choice of n_f and Λ, for fixed $M = 10$ GeV and various values of x_F. The thicker lines correspond to our default choice $n_f = 3$ and $\Lambda = \Lambda^{(3)}_{\overline{\rm MS}} = 0.346$ GeV, whereas the thinner ones correspond to $n_f = 1$ and $\Lambda = \Lambda^{(1)}_{\overline{\rm MS}} = 0.241$ GeV (other notations as in Figs. 5 and 6).

Eqs. (39)–(41)), and therefore the main uncertainties coming from the extrapolation of the perturbative expression of the instanton-size distribution cancel in them. Therefore, it is expected that our predictions of the coefficient functions remain also valid at smallish, but nonzero r. For very small $q_\perp = Mr$, namely up to around 1 GeV, the simplest perturbative and instanton-induced sub-process $q\bar{q} \to \gamma^*$ contributes and may change the angular distributions.

(v) One feature of $\hat{\lambda}^{(\rm pt)}$ and $\hat{\nu}^{(\rm pt)}$ that translates unchanged even to the hadron level is the scaling behavior: they depend only on the ratio r. This is not the case when instanton effects are included since they vanish in comparison to the perturbative contributions for larger M^2. This is basically triggered by the ratio $\hat{\sigma}^{(\rm I)}/\hat{\sigma}^{(\rm pt)}$ which leads to a M^2 dependent weighting of the perturbative and instanton contribution. In addition, also $\hat{\lambda}^{(\rm I)}$ and $\hat{\nu}^{(\rm I)}$ depend already slightly on M^2.

(vi) Remarkable is also the behavior for $x_F = 0$. For vanishing $q_\perp$, one expects to recover the well-known leading-order angular distribution $\propto (1 + \cos^2\theta)$, that is $\hat{\lambda} = 1$ and $\hat{\nu}, \hat{\mu} = 0$. As one can see from Fig. 5 and 6, the function $\hat{\nu}$ tends towards 2. Note that $\hat{\nu}$ still vanishes in the limit $q_\perp \to 0$ for very small but finite x_F. For large x_F, the violation of the Lam–Tung relation is suppressed even in a region where the ratio $\hat{\sigma}^{(\rm I)}/\hat{\sigma}^{(\rm pt)}$ is not small. The very strong x_F dependence will disappear after folding with the parton distributions as we will see in the next section.

Strictly speaking, we should take $n_f = 1$ and a corresponding $\Lambda = \Lambda^{(1)}_{\overline{\rm MS}}$ value for the calculation of the effective coupling parameters b, Eq. (10), and $\xi^{(\rm I)}$, Eq. (29), of the instanton contribution to the helicity structure functions, since our instanton-induced process corresponds to (the

unrealistic case of) one massless flavour, the other flavours being integrated out. In the numerical results shown in Figs. 5 and 6 we have chosen, instead, $n_f = 3$, and $\Lambda = \Lambda^{(3)}_{\overline{\rm MS}} = 0.346$ GeV, for the calculation of the effective coupling parameters $\xi^{(\rm pt)}$, $\xi^{(\rm I)}$, and b. This value of Λ corresponds—according to the standard three-loop perturbative flavour reduction—to an $n_f = 5$ value $\Lambda^{(5)}_{\overline{\rm MS}} = 0.219$ GeV, leading to a running QCD coupling $\alpha_s(m_Z) = 0.119$ at the Z-boson mass [14]. As illustrated in Fig. 7, our results for the coefficient functions are not largely affected if we choose instead the nominal value $n_f = 1$ and a corresponding value for the Λ parameter, $\Lambda^{(1)}_{\overline{\rm MS}} = 0.241$ GeV. This value was obtained by a linear interpolation between the central values found in recent lattice investigations for $n_f = 0$, $\Lambda^{(0)}_{\overline{\rm MS}} = 0.237$ GeV [40], and $n_f = 2$, $\Lambda^{(2)}_{\overline{\rm MS}} = 0.245$ GeV [41]. Again, such details cancel to a great extend in the ratios of structure functions. This also refers to the dependence on the renormalization scale μ_r, for which we have chosen M in the numerical results presented in Figs. 5 and 6.

3.2. Hadron level

Since we have to deal with collisions of hadrons, the partonic Mandelstam variables s, t, u in Eqs. (24)–(28) are not observable. Firstly, we have to calculate the tensor (12) on the hadron level which involves a folding with the usual parton distributions, see, e.g., Ref. [42],

$$W_{\mu\nu}(S,T,U) = \frac{16\pi}{3}\int \frac{{\rm d}x_1}{x_1}\frac{{\rm d}x_2}{x_2} S \sum_i w^{q_i}_{\mu\nu}(s,t,u)\big(q_i(x_1)\bar q_i(x_2) + \bar q_i(x_1) q_i(x_2)\big) \tag{56}$$

$$= \frac{8\pi}{3}\int \frac{{\rm d}x_1}{x_1}\frac{{\rm d}x_2}{x_2}\delta\left(\frac{s+t+u-M^2}{S}\right)\sum_i w'^{q_i}_{\mu\nu}(s,t,u)\big(q_i(x_1)\bar q_i(x_2) + \bar q_i(x_1) q_i(x_2)\big), \tag{57}$$

where the flavour dependence of $w_{\mu\nu}$ is given by the relative charge e_{q_i} in $\xi^{(\rm I)}$ (29) and $\xi^{(\rm pt)}$ (36). Note that the second equation (57) only holds for one parton in the final state, whereas the first equation is applicable for the general partonic tensor (12). The factors entering the hadronic tensor (57) are fixed in such a way that the tensor fits with the one defined in [42].[6] We have to project the hadronic tensor (57) now on the hadron momenta K_1 and K_2 to get the accessible hadronic structure functions W_i,

$$W_{\mu\nu} = -\tilde g_{\mu\nu} W_1 + \tilde K_\mu \tilde K_\nu W_2 - \frac{\tilde K_\mu \tilde k_\nu + \tilde K_\nu \tilde k_\mu}{2} W_3 + \tilde k_\mu \tilde k_\nu W_4. \tag{58}$$

Here we have defined, similar to the partonic case discussed before, the vectors, $K = K_1 + K_2$, $k = K_1 - K_2$, $\tilde K_\mu = \tilde g_{\mu\nu} K^\nu/\sqrt{S}$ and $\tilde k_\mu = \tilde g_{\mu\nu} k^\nu/\sqrt{S}$. Note the differences between the partonic momenta k', K' and the hadronic ones k, K in the hadronic tensor (58). Due to the different projections on the hadron level the hadron structure function W_i is a linear combination of foldings of the four partonic functions w'_i with the parton distributions. Using the partonic functions (25)–(28) for the instanton-induced contribution and Eqs. (32)–(35) for the perturbative one, we have now everything at hand to calculate the observable angular distributions (39)–(41) on the hadron level.

[6] Constant factors are for our purposes actually not important since we are only interested in ratios of functions W_i.

For fixed M, the angular distributions on the partonic level depend only on r and x_F, but they are independent of the center-of-mass (c.m.) energy $\sqrt{s}$, because the latter is fixed due to the relation $s + t + u = M^2$. On the hadron level, however, the momentum fractions x_1 and x_2 are variable, and the angular distributions depend, correspondingly, for fixed M, on the hadronic c.m. energy $\sqrt{S}$. Furthermore, the variable x_F has to be replaced by the hadronic one,

$$X_F = \frac{T - U}{S}, \tag{59}$$

which can be interpreted as the longitudinal photon-momentum fraction with respect to the momentum of the hadron h_1.

Fig. 8 shows the resulting angular distributions for proton–proton collisions at $\sqrt{S} = 15$ GeV for $M = 7$ GeV, $X_F = 0, 0.1, 0.3$, and varying values of $r = q_\perp/M$. For the renormalization scale we have chosen $\mu_r = M$ and for the parton distributions the CTEQ6 dataset [43].[7]

The main difference to the partonic quantities, shown in Fig. 5, concerns the x_F respectively X_F dependence. The strong x_F dependence is smeared out on the hadron level. This smearing leads in particular to a suppression of the instanton-induced effect at small X_F. This has nothing to do with the parton distribution functions entering the hadronic angular distribution. Actually, since the angular distributions are *ratios* of two foldings with parton distribution functions, their dependence on the type of hadrons in the initial states is rather weak. The difference is just a consequence of the $x_{1,2}$ dependence of the partonic Feynman variable x_F that leads to the smeared out X_F behavior after integrating over $x_{1,2}$. For similar reasons, the M^2 dependence of the angular distribution in the instanton background is stronger than on the parton level, since for smaller ratios M^2/s also smaller values of x_F contribute, see Figs. 8 and 9; but note that due to kinematical reasons only smaller values of $r = q_\perp/M$ are accessible for larger ratios M^2/s.

The fiducial region of instanton perturbation theory on the parton level $\sqrt{-t}, \sqrt{-u}, M > \mathcal{Q}_{\min} \approx (4\text{–}6)$ GeV can be mapped on the hadronic variables. One can check that theses relations are fulfilled for all x_1 and x_2 for large enough values of M and $q_\perp$, namely $M \geqslant \mathcal{Q}_{\min}$ and $q_\perp \gtrsim \mathcal{Q}_{\min}$. Also on the hadron level our results should hold for even smaller $q_\perp$, since the uncertainty towards smaller $q_\perp$ drops out in the ratios of the angular distributions, see the discussion in Section 3.1.

3.3. More partons in the final state

As already mentioned in the introduction, the discussed instanton-induced sub-process $q\bar{q} \xrightarrow{I} \gamma^* g$ with only one gluon and no quarks in the final state is quite instructive since it contains already the basic nontrivial feature of the instanton-induced Drell–Yan process, namely the helicity flip of the quarks in the initial state, which is related to the chirality violation and is essentially responsible for the violation of the Lam–Tung relation [22,29]. But the rate of this asymmetry induced by instantons was certainly underestimated in the previous sections since it is well known that the resummation of the events with an arbitrary number of final-state gluons leads to a large enhancement which eats up at least partially the suppression of the instanton-induced process $q\bar{q} \to \gamma^* g$. In addition, also the number of involved quarks in the subprocess is not realistic, see Section 2.

[7] Actually a consistent treatment of instanton induced effects requires also parton distributions including instanton-induced parton evolution. Since this modification enters the perturbative and instanton contribution in the same way this effect would change the angular distribution only in sub-leading order of instanton perturbation theory.

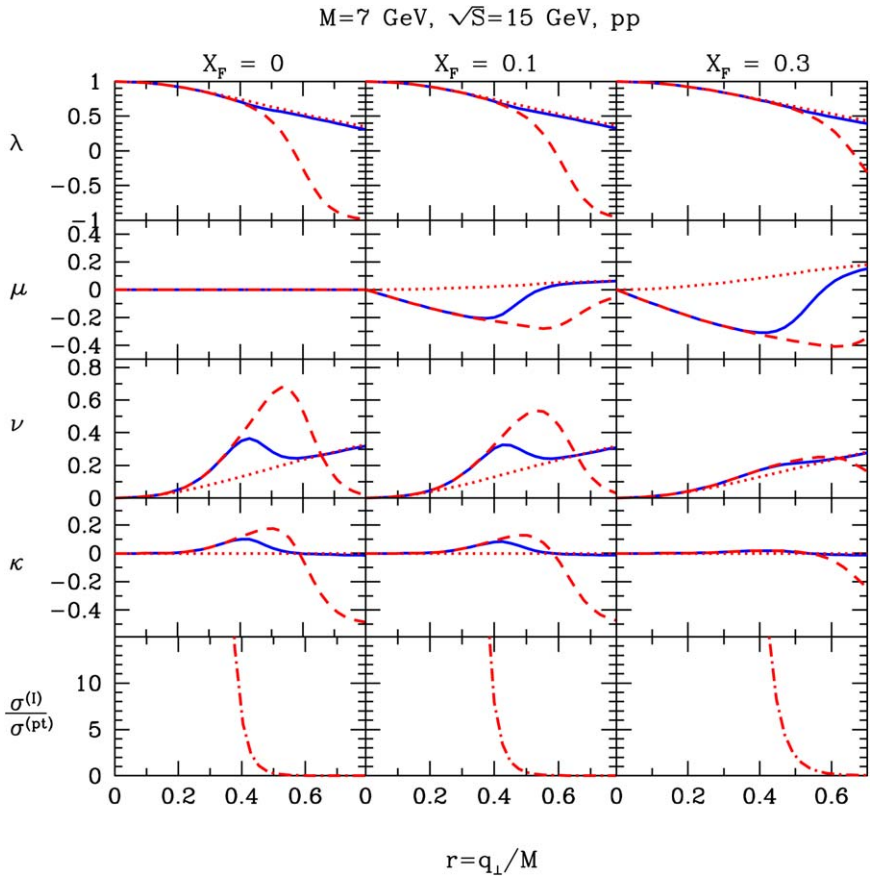

Fig. 8. The plot shows the angular structure functions similar to Fig. 5 but on hadron level. Therefore an integration over parton distributions, e.g., for the proton, is included. Due to the variable momentum fractions x_1 and x_2 one has to specify an additional kinetic variable, e.g., the c.m. energy $\sqrt{S}$.

A complete calculation of the angular distribution for this general instanton-induced process is beyond the scope of this paper and will be attempted in the future. Let us roughly sketch the general features of the complete process. Whereas in perturbative processes additional final-state gluons are certainly suppressed by an order of α_s, every additional gluon in an instanton background leads to an *enhancement* of the order $1/\alpha_s$. Summing over all processes with an arbitrary number of gluons n_g leads to an exponentiation of the inverse coupling constant. The resulting factor, combined with the tunneling factor, $\exp[-4\pi/\alpha_s]$ (cf., e.g., Eq. (29)), can be written as $\exp[-4\pi/\alpha_s F(x')]$. Here, the Bjorken scaling variable $x' = \mathcal{Q}^2/(\mathcal{Q}^2 + M_X^2)$ appears, where $\mathcal{Q}$ is the relevant momentum transfer and M_X is the invariant mass of the produced partonic final state. The so-called holy-grail function $F(x')$ [8] is normalized to one for $x' = 1$ and decreases towards smaller x' and therefore larger M_X. Let us mention that in the electroweak theory, where the coupling constant is much smaller, this mechanism is absolutely necessary for the process eventually becoming observable in the high energy limit [7].

For the process discussed in the present paper, $\mathcal{Q}^2$ is given by the partonic quantities $-t$, $-u$ or M^2, whereas, in general, $M_X^2 = (k_1 + k_2 - q)^2$. Therefore, the integrands of the functions

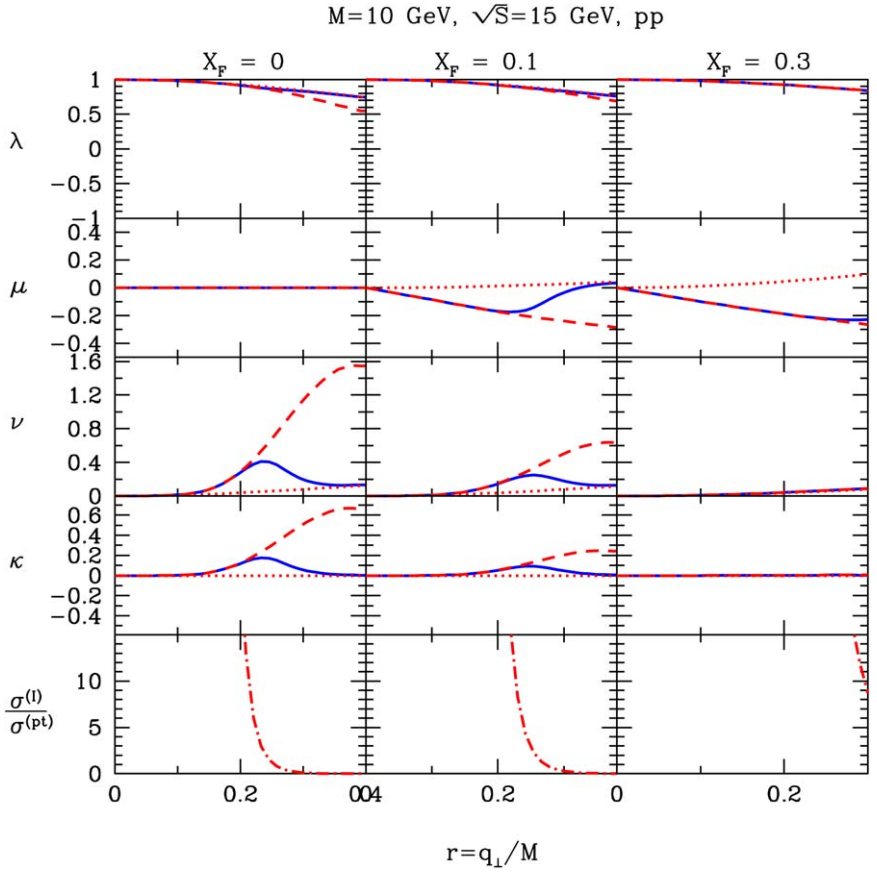

Fig. 9. Same as in Fig. 8, but for $M = 10$ GeV.

W_i (57) involve a factor $\exp[-4\pi/\alpha_s F(x')]$. For $M_X^2 = 0$ ($x' = 1$), and therefore also for the process with one final-state gluon, the factor $\exp[-4\pi/\alpha_s]$ in Eq. (29) is recovered. For positive X_F, the smallest x' is given for $\mathcal{Q}^2 = -t$,

$$x' = \frac{-t}{-t + M_X^2} = \frac{-t}{s + u - M^2} = \frac{-2M^2/S + x_1(\sqrt{4M^2/S(1+r^2) + X_F^2} - X_F)}{2x_2 x_1 - x_2(\sqrt{4M^2/S(1+r^2) + X_F^2} + X_F)}. \quad (60)$$

It is easy to check that x' rises slightly with r and decreases towards the largest accessible values of X_F. Therefore, we can conclude that the instanton-induced effect in ν and κ (see Figs. 5, 6, 8 and 9) will shift to slightly smaller r. Furthermore, we expect a significant enhancement of the instanton effect for larger X_F. Correspondingly, the suppression of the simplest instanton-induced process at large X_F, which we observed before, might be compensated. Note that the applicability of instanton perturbation-theory now requires in addition a cut $x' \gtrsim x_{\text{cut}}$, where x_{cut} is approximately 0.35, see Ref. [36]. One can check that this requirement can be fulfilled for all x_1, x_2 and r as long as X_F is not too large, or for all X_F for large enough ratios M^2/S.

Beside the discussed instanton-induced multi-gluon process also other perturbative processes may contribute. Firstly, we have not taken into account an enhancement of perturbative contribu-

tions due to soft gluon resummation [24,25] at small $q_\perp$ since the instanton-induced contribution that we have calculated is not reliable in this region anyway. In higher order α_s also new processes contribute to the angular distribution which lead to a small violation of the Lam–Tung relation already in the purely perturbative framework [23]. For small transverse momenta $q_\perp$ the usual factorization is not reliable anymore and transverse parton momentum distributions become important. However, as already mentioned in the introduction, higher order contributions, soft gluon effects and parton transverse momentum are not able to explain the observed strong violation of the Lam–Tung relation [23–25].

4. Conclusions

We have calculated the angular distribution of the produced leptons in hadron–hadron collision in an instanton background. It turns out that, for large enough photon virtualities M^2 and transverse photon momenta squared $q_\perp^2$, only small instantons contribute. Therefore, the instanton-induced contribution is fiducially calculable in this kinematic region using techniques of instanton perturbation theory. The most remarkable property of the resulting angular distribution is the violation of the Lam–Tung relation which is conserved to very high accuracy in usual perturbation theory, but violated in experiments. This effect is a direct consequence of chirality violation in the background of QCD instantons which leads to a nontrivial spin-density of the quark–antiquark pair in the initial state as it has been argued in [29]. Therefore, lepton pair production in hadron collisions is potentially a very good testing ground for instanton-induced processes: the violation of the Lam–Tung relation is reliably calculable in instanton perturbation theory and absent in usual perturbation theory.

We restricted ourselves to the simplest partonic subprocess $q\bar{q} \xrightarrow{I} \gamma^* + g$. Since the inclusion of the more realistic general processes $q\bar{q} \xrightarrow{I} \gamma^* + (n_f - 1)q\bar{q} + n_g g$ was beyond the scope of this paper, we cannot compare our results directly with the available data. However, the small violation of the Lam–Tung relation on the hadron level arising from the simplest partonic process is already quite promising, notably in view of the expectation that additional gluons lead to a substantial enhancement of the instanton-induced effect, as known from analyses of the related processes in deep-inelastic scattering and from the general arguments presented in this paper.

Finally, let us mention that, beside further theoretical efforts, more experimental data are required for testing instantons in the angular distribution of produced leptons at a hadron collider. Fortunately, there are new medium energy projects under way that are also dedicated to study the Drell–Yan process, e.g., at the forthcoming facilities GSI-FAIR [44] and J-PARC [45].[8] Experiments at RHIC may also give further information on lepton pair production. In general, it seems that fixed target experiments are especially well suited for our purposes, since on the one hand the involved momenta are smaller and on the other hand the luminosities are larger. Therefore, a huge amount of lepton pairs should be observable which is absolutely necessary for reconstructing a whole angular distribution.

[8] At J-PARC a proton beam of 50 GeV ($\sqrt{S} \approx 10$ GeV) will be used for fixed target experiments and at the FAIR experiment a 29 GeV antiproton beam will be available for fixed target experiments or collisions with low energy protons ($\sqrt{S} \approx 6$–15 GeV). Clearly, proton–antiproton collisions are perfectly suited for studying Drell–Yan since the rate is higher as in proton–proton collisions.

Acknowledgements

One of us (A.R.) would like to thank Sven Moch and Fridger Schrempp for sharing their insights into QCD instanton-induced hard scattering processes with him. A.U. would like to thank Fridger Schrempp for countless illuminating discussions about instantons and beyond. A.B. and A.U. would like to thank also Otto Nachtmann and Daniël Boer for numerous discussions about lepton pair production in hadron collisions as a testing ground for perturbative QCD. We thank also Markus Diehl for valuable information on future experiments on Drell–Yan production. The work of A.B. was partially supported by a Heisenberg grant of the Deutsche Forschungsgemeinschaft. The work of A.U. was supported by the research program of the "Stichting voor Fundamenteel Onderzoek der Materie (FOM)", which is financially supported by the "Nederlandse Organisatie voor Wetenschappelijk Onderzoek (NWO)".

References

[1] S.L. Adler, Phys. Rev. 177 (1969) 2426;
J.S. Bell, R. Jackiw, Nuovo Cimento A 60 (1969) 47;
W.A. Bardeen, Phys. Rev. 184 (1969) 1848.
[2] G. 't Hooft, Phys. Rev. Lett. 37 (1976) 8;
G. 't Hooft, Phys. Rev. D 14 (1976) 3432;
G. 't Hooft, Phys. Rev. D 18 (1978) 2199, Erratum.
[3] A. Belavin, A. Polyakov, A. Shvarts, Y. Tyupkin, Phys. Lett. B 59 (1975) 85.
[4] E.V. Shuryak, Nucl. Phys. B 203 (1982) 93;
D. Diakonov, V.Y. Petrov, Phys. Lett. B 147 (1984) 351;
D. Diakonov, V.Y. Petrov, Nucl. Phys. B 272 (1986) 457;
T. Schäfer, E.V. Shuryak, Rev. Mod. Phys. 70 (1998) 323;
D. Diakonov, Prog. Part. Nucl. Phys. 51 (2003) 173.
[5] F.R. Klinkhamer, N.S. Manton, Phys. Rev. D 30 (1984) 2212;
V.A. Kuzmin, V.A. Rubakov, M.E. Shaposhnikov, Phys. Lett. B 155 (1985) 36;
P. Arnold, L.D. McLerran, Phys. Rev. D 36 (1987) 581;
A. Ringwald, Phys. Lett. B 201 (1988) 510.
[6] V.A. Rubakov, M.E. Shaposhnikov, Usp. Fiz. Nauk 166 (1996) 493, Phys. Usp. 39 (1996) 461.
[7] H. Aoyama, H. Goldberg, Phys. Lett. B 188 (1987) 506;
A. Ringwald, Nucl. Phys. B 330 (1990) 1;
O. Espinosa, Nucl. Phys. B 343 (1990) 310;
V.V. Khoze, A. Ringwald, Phys. Lett. B 259 (1991) 106.
[8] L.D. McLerran, A.I. Vainshtein, M.B. Voloshin, Phys. Rev. D 42 (1990) 171;
J.M. Cornwall, Phys. Lett. B 243 (1990) 271;
P.B. Arnold, M.P. Mattis, Phys. Rev. D 42 (1990) 1738;
S.Y. Khlebnikov, V.A. Rubakov, P.G. Tinyakov, Nucl. Phys. B 350 (1991) 441;
A.H. Mueller, Nucl. Phys. B 348 (1991) 310;
A.H. Mueller, Nucl. Phys. B 353 (1991) 44;
V.V. Khoze, A. Ringwald, Nucl. Phys. B 355 (1991) 351.
[9] G.R. Farrar, R.-B. Meng, Phys. Rev. Lett. 65 (1990) 3377;
A. Ringwald, F. Schrempp, C. Wetterich, Nucl. Phys. B 365 (1991) 3;
M.J. Gibbs, A. Ringwald, B.R. Webber, J.T. Zadrozny, Z. Phys. C 66 (1995) 285;
D.A. Morris, A. Ringwald, Astropart. Phys. 2 (1994) 43;
Z. Fodor, S.D. Katz, A. Ringwald, H. Tu, Phys. Lett. B 561 (2003) 191;
T. Han, D. Hooper, Phys. Lett. B 582 (2004) 21;
M. Ahlers, A. Ringwald, H. Tu, Astropart. Phys. 24 (2006) 438.
[10] A. Ringwald, Phys. Lett. B 555 (2003) 227;
F. Bezrukov, D. Levkov, C. Rebbi, V.A. Rubakov, P. Tinyakov, Phys. Rev. D 68 (2003) 036005;
A. Ringwald, JHEP 0310 (2003) 008.

[11] I.I. Balitsky, V.M. Braun, Phys. Lett. B 314 (1993) 237;
A. Ringwald, F. Schrempp, in: Quarks '94, Vladimir, Russia, 1994, hep-ph/9411217.
[12] S. Moch, A. Ringwald, F. Schrempp, Nucl. Phys. B 507 (1997) 134.
[13] A. Ringwald, F. Schrempp, Phys. Lett. B 438 (1998) 217.
[14] A. Ringwald, F. Schrempp, Comput. Phys. Commun. 132 (2000) 267.
[15] H1 Collaboration, C. Adloff, et al., Eur. Phys. J. C 25 (2002) 495;
ZEUS Collaboration, S. Chekanov, et al., Eur. Phys. J. C 34 (2004) 255.
[16] D.E. Kharzeev, Y.V. Kovchegov, E. Levin, Nucl. Phys. A 690 (2001) 621;
M.A. Nowak, E.V. Shuryak, I. Zahed, Phys. Rev. D 64 (2001) 034008;
F. Schrempp, J. Phys. G 28 (2002) 915;
F. Schrempp, A. Utermann, Acta Phys. Pol. B 33 (2002) 3633;
F. Schrempp, A. Utermann, Phys. Lett. B 543 (2002) 197;
F. Schrempp, A. Utermann, hep-ph/0301177;
F. Schrempp, A. Utermann, hep-ph/0401137;
F. Schrempp, A. Utermann, hep-ph/0407146.
[17] F. Schrempp, in: A. De Roeck, H. Jung (Eds.), Proc. HERA and the LHC—A Workshop on the Implications of HERA for LHC Physics, CERN-2005-014, p. 1, hep-ph/0407146.
[18] M. Petermann, F. Schrempp, in preparation;
M. Petermann, PhD thesis, in preparation.
[19] S.D. Drell, T.M. Yan, Phys. Rev. Lett. 25 (1970) 316;
S.D. Drell, T.M. Yan, Phys. Rev. Lett. 25 (1970) 902, Erratum.
[20] J.R. Ellis, M.K. Gaillard, W.J. Zakrzewski, Phys. Lett. B 81 (1979) 224.
[21] C.S. Lam, W.K. Tung, Phys. Rev. D 21 (1980) 2712.
[22] A. Brandenburg, O. Nachtmann, E. Mirkes, Z. Phys. C 60 (1993) 697.
[23] E. Mirkes, J. Ohnemus, Phys. Rev. D 51 (1995) 4891.
[24] P. Chiappetta, M. Le Bellac, Z. Phys. C 32 (1986) 521.
[25] D. Boer, W. Vogelsang, hep-ph/0604177.
[26] NA10 Collaboration, S. Falciano, et al., Z. Phys. C 31 (1986) 513.
[27] NA10 Collaboration, M. Guanziroli, et al., Z. Phys. C 37 (1988) 545.
[28] J.S. Conway, et al., Phys. Rev. D 39 (1989) 92.
[29] D. Boer, A. Brandenburg, O. Nachtmann, A. Utermann, Eur. Phys. J. C 40 (2005) 55.
[30] C.W. Bernard, Phys. Rev. D 19 (1979) 3013.
[31] T.R. Morris, D.A. Ross, C.T. Sachrajda, Nucl. Phys. B 255 (1985) 115.
[32] A. Hasenfratz, P. Hasenfratz, Nucl. Phys. B 193 (1981) 210.
[33] M. Lüscher, Nucl. Phys. B 205 (1982) 483.
[34] G. 't Hooft, Phys. Rep. 142 (1986) 357.
[35] UKQCD Collaboration, D.A. Smith, M.J. Teper, Phys. Rev. D 58 (1998) 014505.
[36] A. Ringwald, F. Schrempp, Phys. Lett. B 459 (1999) 249;
A. Ringwald, F. Schrempp, Phys. Lett. B 503 (2001) 331.
[37] J.A.M. Vermaseren, math-ph/0010025.
[38] J.C. Collins, D.E. Soper, Phys. Rev. D 16 (1977) 2219.
[39] C.S. Lam, W.K. Tung, Phys. Rev. D 18 (1978) 2447.
[40] ALPHA Collaboration, S. Capitani, M. Lüscher, R. Sommer, H. Wittig, Nucl. Phys. B 544 (1999) 669.
[41] ALPHA Collaboration, M. Della Morte, R. Frezzotti, J. Heitger, J. Rolf, R. Sommer, U. Wolff, Nucl. Phys. B 713 (2005) 378.
[42] C.S. Lam, W.K. Tung, Phys. Lett. B 80 (1979) 228.
[43] J. Pumplin, D.R. Stump, J. Huston, H.L. Lai, P. Nadolsky, W.K. Tung, JHEP 0207 (2002) 012.
[44] PAX Collaboration, Antiproton–proton scattering experiments with polarization, Letter of Intent, Darmstadt, 2004, available at http://www.fz-juelich.de/ikp/pax.
[45] More information about the Japan Proton Accelerator Research Complex (J-PARC) are available at http://j-parc.jp/NuclPart/index_e.html.